Journal of Neurology (2019) 266:1474–1480
https://doi.org/10.1007/s00415-019-09284-2

ORIGINAL COMMUNICATION

Brain white matter changes in asymptomatic carriers of Leber's hereditary optic neuropathy

Miaomiao Long[1,2] · Ling Wang[3,4] · Qin Tian[3,4] · Hao Ding[1] · Wen Qin[1] · Dapeng Shi[3,4] · Chunshui Yu[1]

Received: 3 January 2019 / Revised: 13 March 2019 / Accepted: 15 March 2019 / Published online: 25 March 2019

Abstract

Objective Subclinical abnormalities, including microangiopathy, swelling of nerve fibers, visual field abnormalities and visual functional impairments had been reported in Leber's hereditary optic neuropathy (LHON) carriers. The purpose of this study was to investigate microstructural changes of brain white matter in asymptomatic LHON carriers using DTI and tract-based spatial statistics (TBSS).

Methods DTI and neuro-ophthalmologic measurements were acquired in 14 LHON carriers and 15 gender- and age-matched healthy controls, and diffusion metrics, including fractional anisotropy (FA), axial (AD), radial diffusion (RD) and mean diffusion (MD) were calculated. Intergroup differences in diffusion metrics were compared regressing out potential nuisance covariates of age and gender. A correlation analysis was performed to test associations between abnormal neuro-ophthalmologic measures and diffusion metrics while controlling the effects of age and gender.

Results Compared to healthy controls, LHON carriers showed a weak increase of thickness of the retinal nerve fiber layer (RNFL) of the right inferior quadrant ($F = 5.22$, $p = 0.032$, before multiple comparison correction). LHON carriers exhibited widespread decreased FA value (bilateral anterior thalamic radiations, bilateral corticospinal tracts, major and minor forceps, bilateral inferior fronto-occipital fasciculi and left superior longitudinal fasciculus), increased RD value (bilateral anterior thalamic radiations, bilateral corticospinal tracts, major and minor forceps, bilateral inferior fronto-occipital fasciculi, bilateral inferior longitudinal fasciculi, bilateral superior longitudinal fasciculi and bilateral uncinate fasciculi) and increased MD value (bilateral anterior thalamic radiations, bilateral corticospinal tracts, minor forceps, bilateral inferior fronto-occipital fasciculi, bilateral inferior longitudinal fasciculi, left superior longitudinal fasciculus and bilateral uncinate fasciculi). Moreover, these changed diffusion metrics were not correlated with age, gender, LHON mutations and retinal measures in LHON carriers.

Conclusion Our results show microstructural alterations in brain white matter in asymptomatic LHON carriers, indicating that LHON-related genetic mutations themselves might result in occult white matter alterations in the brain.

Keywords Leber's hereditary optic neuropathy · Diffusion tensor imaging · Tract-based spatial statistics · Retinal nerve fiber layer · White matter · Carriers

Abbreviations

AD	Axial diffusivity
RD	Radial diffusivity
FA	Fractional anisotropy
TBSS	Tract-based spatial statistics
LHON	Leber's hereditary optic neuropathy

✉ Wen Qin
wayne.wenqin@gmail.com

✉ Dapeng Shi
cjr.shidapeng@vip.163.com

✉ Chunshui Yu
chunshuiyu@tmu.edu.cn

[1] Department of Radiology and Tianjin Key Laboratory of Functional Imaging, Tianjin Medical University General Hospital, No. 154, Anshan Road, Heping District, Tianjin 300052, China

[2] Department of Radiology, Tianjin First Central Hospital, Tianjin 300192, China

[3] Department of Radiology, Zhengzhou University People's Hospital, Henan Provincial People's Hospital, Zhengzhou 450003, Henan, China

[4] Henan Key Laboratory for Medical Imaging of Neurological Disease, Zhengzhou 450003, Henan, China

mtDNA Mitochondrial DNA
RNFL Retinal nerve fiber layer

Introduction

Leber's hereditary optic neuropathy (LHON) is a maternally inherited genetic disease with young male predilection and characterized by an acute or subacute bilateral sequential loss of central vision [18, 37, 55]. It has been linked to mitochondrial DNA (mtDNA) mutations that would affect oxidative phosphorylation in mitochondria [21, 28, 32]. LHON shows retinal ganglion cell degeneration and axonal loss of the optic nerve that could be identified by measuring the thickness of RNFL. The small caliber fibers of the papillomacular bundle are lost selectively at an early stage, and then the involvement of the rest of fibers results in optic nerve atrophy, which usually occurs at an advanced stage of the disease [48]. Consistent with clinical and pathological features, MRI studies have demonstrated atrophy and increased T2 signals in the optic nerves in LHON patients [23].

Besides the involvement of the optic nerves, a small percent of LHON patients also show neurological signs, including but not limited to dystonia [34, 39], parkinsonism [39], cerebellar ataxia [12, 36], epilepsy [6, 13], myoclonus [8, 25], migraine [6, 25],intellectual disability [6],auditory dysfunction [45], suggesting the involvement of the brain. As a special clinical pattern of LHON, Leber plus has been reported to be indistinguishable from a brain disorder of multiple sclerosis [16]. The structural damage of the visual cortex and retinofugal pathway has been reported in chronic LHON patients, which could be related to axonal degeneration secondary to the loss of retinal ganglion cells [4, 35]. Although LHON patients have brain damage outside the visual pathway [33, 47], it is still unknown whether LHON mutations have a direct impact on brain structural properties.

A variety of biological changes have been reported in asymptomatic LHON carriers. For example, the mtDNA/nuclear DNA content is increased in asymptomatic LHON carriers but not in LHON patients, indicating a possible mechanism that protects carriers from progressing into LHON [40]. As a useful indicator of neuronal distress [22, 57], the serum neuron-specific enolase is elevated in asymptomatic LHON carriers than in LHON patients, and the increase in neuron-specific enolase is more prominent in male than in female carriers [58]. Clinically, LHON carriers show the thickening of the RNFL [50], dysfunction of retinal elements [49] and luminance and chromatic spatial contrast sensitivity losses [53]. For limited MR report of carriers, increased Cho concentration, Cho/Cr ratio and decreased absolute NAA concentration were reported in white matter lesions of a 26-year-old female asymptomatic LHON mutation carrier with bilateral periatrial lesions [19]. Decrease of the absolute concentration of creatine and *N*-acetylaspartate to creatine ratio in normal-appearing white matter [42], and increase of cortical thickness in visual cortex (V2 and V3) [9] were reported in case–control studies.

Despite the lack of direct evidence, we hypothesize that changes in oxygen consumption [54], antioxidants [24], phosphorylation and mitochondrial ATP production [30, 31] secondary to mtDNA mutations might result in brain white matter (WM) alterations in asymptomatic LHON carriers. Since DTI is a promising technique for measuring WM changes of the brain [26, 27], in this study, we acquired DTI data from 14 LHON carriers and explored potential changes of fractional anisotropy (FA) using a voxel-wise tract-based spatial statistics (TBSS) [51]. We also calculated axial diffusivity and radial diffusivity to elucidate the mechanism of FA changes, and to explain the possible underlying pathological changes of the compromised WM tracts [44, 56]. Finally, we tested the potential associations between clinical retinal measures and WM diffusion metrics in LHON carriers.

Subjects and methods

Participants

We prospectively recruited 14 LHON carriers without clinical symptoms from siblings, cousins or parents of LHON patients who were diagnosed at the Zhengzhou University People's Hospital from May 2012 to December 2016. Inclusion criteria were: (1) with one of the three main point mutations of mtDNA associated with LHON (m.3460G > A, m.11778G > A, m.14484T > C); (2) no ophthalmic abnormalities confirmed by careful ophthalmic examinations; (3) no history of neurological, psychiatric, major medical conditions, or substance abuse; (4) no intracranial or intraorbital lesions on routine MR images. We also recruited 15 gender- and age-matched healthy controls. The inclusion criteria were the same as LHON carriers except for point mutations of mtDNA associated with LHON.

Neuro-ophthalmologic assessment

The best-corrected visual acuity was assessed by the logarithm of the minimum angle of resolution (logMAR) notation performed with high-intensity red-free light. The visual field was assessed using Octopus perimeter101G2 program TOP Strategy (Interzeag AG, Haig-Streit Schlieren, Switzerland) and the mean sensitivity, mean defect, and loss of variance were quantified. The average thicknesses of the peripapillary RNFL (360° measure) and four quadrant RNFL (superior, inferior, nasal and temporal) were measured by a high-resolution spectral-domain optical coherence

tomography (Carl Zeiss Meditec, Dublin, CA, USA). The RNFL thickness was measured by a trained technician using circumpapillary scans centered on the optic nerve disk, with a preset diameter of 3.45 mm.

MRI data acquisition

Brain MRI data were obtained by a 3.0T MR scanner (Discovery MR750, GE Healthcare, Waukesha, WI, USA). Tight foam padding was used to minimize head motion, and earplugs were used to reduce noise. The routine MRI scans of brain and orbit were performed to exclude visible abnormalities. Structural T1w volumes were acquired by fast-spoiled gradient recalled imaging (TE = 3.2 ms, TR = 8.2 ms, FOV = 256 mm × 256 mm; matrix size = 256 × 256, slice thickness = 1 mm without gap, and 188 slices). DTI data were acquired using a diffusion-weighted spin-echo single-shot EPI sequence with 1 non-diffusion-weighted image and 30 diffusion encoding directions ($b = 1000$s/mm^2). The scan parameters were TE = 90 ms, TR = 8000 ms, FOV = 240 mm × 240 mm, matrix size = 128 × 128, slice thickness = 3 mm without gap, and 48 slices.

Data preprocessing

DTI data were preprocessed according to the pipelines of the FMRIB's Diffusion Toolbox (FDT) implemented in FSL 5.0.10 (FDT tool, FSL 5.0.10, http://www.fmrib.ox.ac.uk). First, eddy-current-induced distortions and head motion were corrected using the eddy correct toolbox [17]. Then, brain tissue was extracted using brain extract toolbox (version 2.1). The diffusion tensor was fitted using a linear least square algorithm and eigenvalues were decomposed from the tensor to calculate diffusion metrics of the FA, AD and RD [5].

TBSS analysis

Intergroup differences of FA, AD, RD and MD were investigated with a modified TBSS pipeline: (1) the individual FA, AD, RD and MD maps were first rigidly aligned to Montreal Neurological Institute (MNI) space using a default FMRIB58_FA atlas by the fMRI of the Brain Linear Image Registration Tool (FLIRT; https://fsl.fmrib.ox.ac.uk/fsl/fslwiki/FLIRT) with 12-parameter model, then jointly registered using SPM12 software (http://www.fil.ion.ucl.ac.uk/spm/software/spm12) with diffeomorphic anatomical registration via an exponential Lie algebra (DARTEL) algorithm to a study-specific template generated with data from all study participants. (2) The normalized FA maps were averaged to generate a group-wise white matter skeleton using a center-of-gravity algorithm; (3) the group-wise skeleton was refined to contain only the backbone of white matter using a threshold of FA > 0.2; (4) the individual FA skeleton map was generated by projecting the normalized individual FA map onto the group-wise skeleton mask; and (5) individual AD, RD and MD skeleton maps were also created using the same projection parameters [51]. A general linear model was performed to compare voxel-wise differences of FA, AD, RD and MD between LHON carriers and healthy controls with a non-parametric permutation-based inference (''randomize'' program within FSL) with age and gender as covariates [38]. The number of permutations was set to 5000. For significant neuro-ophthalmologic measures, voxel-wise correlation with significant diffusion metrics was also performed with the general linear model with "randomize" program within FSL. A family-wise error method ($P < 0.05$) was used to correct for multiple comparison using the threshold-free cluster enhancement option in permutation testing tool in FSL [52].

Statistical analyses for other measures

Two-sample t test was used to test difference in age and Chi-square test or Fisher's exact test was used to test difference of distribution of gender between LHON carriers and healthy controls. An ANOVA analysis regressing out age and gender effects was performed for neuro-ophthalmologic measures ($P < 0.05$). For the RNFL thickness of four quadrants of each eye, adjustment for multiplicity was made by changing the significant P level value to 0.0125.

Results

There were 8 LHON carriers with 11,778 mtDNA mutation, 4 with 14,484 mutation and 2 with 3460 mutation (3 men and 11 women; mean age = 37.1 ± 12.7 years, range = 9–52 years). The age ($t = 1.23$, $P = 0.227$) and gender (Fisher's exact $P = 0.682$) were not significantly different from healthy controls (5 men and 10 women; mean age = 31.9 ± 10.2 years, range = 11–44 years). There were two pediatric subjects in the LHON carrier group (carrier 14: female, 17 years old and carrier 15: female, 9 years old) and one in health control group (control 38: female, 11 year old).

Neuro-ophthalmologic comparisons

An 11-year-old pediatric health control and a 50-year-old LHON carrier refused the neuro-ophthalmologic test. Only the thickness of the right-inferior-quadrant RNFL had intergroup difference before correction for multiple comparisons ($F = 5.22$, $P = 0.032$ Table 1, the meaningful P value level was changed to 0.0125 when performing adjustment for multiplicity). The mean RNFL thickness of the left eye of six LHON carriers (46.15%) and nine health controls (64.29%)

Table 1 Demographic characteristic and visual function of LHON patients and control groups

	Health controls	LHON carriers	*P* value Healthy controls versus LHON carriers
Age	31.87 ± 10.22	37.14 ± 12.73	0.227
Gender	M5F10	M3F11	0.682*
Left eye			
Visual acuity	1.01 ± 0.05	1.03 ± 0.21	0.882
Mean sensitivity	27.19 ± 1.36	26.75 ± 1.46	0.238
Mean defect	1.54 ± 1.27	1.58 ± 1.43	0.736
Loss of variance	4.03 ± 2.48	3.37 ± 2.69	0.557
RNFL			
Average	103 ± 7.96	101.08 ± 8.62	0.633
Temporal	77.21 ± 12.83	69.69 ± 17.01	0.362
Superior	136 ± 13.43	132.54 ± 15.20	0.652
Orbital	64 ± 9.59	65.615 ± 13.44	0.994
Inferior	134.43 ± 17.87	137 ± 15.52	0.714
Right eye			
Visual acuity	1.01 ± 0.05	1.04 ± 0.09	0.786
Mean sensitivity	27.25 ± 0.96	26.74 ± 2.21	0.457
Mean defect	1.49 ± 0.90	1.59 ± 2.01	0.932
Loss of variance	3.93 ± 2.09	5.56 ± 5.80	0.396
RNFL			
Average	101.79 ± 6.93	102.23 ± 7.58	0.899
Temporal	77.57 ± 13.85	74.69 ± 19.21	0.910
Superior	131.36 ± 16.03	124 ± 12.12	0.269
Orbital	68.29 ± 9.08	68.92 ± 14.76	0.602
Inferior	130.14 ± 10.46	141.92 ± 12.93	0.032$^{\Delta}$

*Fisher's exact test

Δp value's meaningful level was 0.0125 to adjust for multiplicity

and the mean RNFL thickness of the right eye of seven LHON carriers (53.85%) and six health controls (42.86%) were greater than 100 μm.

Microstructural changes in brain WM in LHON carriers

In the voxel-wise TBSS analysis, LHON carriers showed widespread decreased FA value (mainly in 9 fibers: bilateral anterior thalamic radiations, bilateral corticospinal tracts, major and minor forceps, bilateral inferior fronto-occipital fasciculi and left superior longitudinal fasciculus), increased RD value(mainly in 14 fibers: bilateral anterior thalamic radiations, bilateral corticospinal tracts, major and minor forceps, bilateral inferior fronto-occipital fasciculi, bilateral inferior longitudinal fasciculi, bilateral superior longitudinal fasciculi and bilateral uncinate fasciculi) and increased MD value (mainly in 12 fibers: bilateral anterior thalamic radiations, bilateral corticospinal tracts, minor forceps, bilateral inferior fronto-occipital fasciculi, bilateral inferior longitudinal fasciculi, left superior longitudinal fasciculus and bilateral uncinate fasciculi) ($P < 0.05$, family-wise error corrected) (Fig. 1). No significant abnormal AD changes were detected and no significant correlation was found between the neuro-ophthalmologic measurements and these diffusion metrics showing intergroup differences in LHON carriers (data not shown).

Discussion

In this study, we used TBSS analysis of DTI data to investigate possible microstructural changes of brain white matter in LHON carriers and their correlations with neuro-ophthalmologic measures. The most important finding is that, compared to healthy controls, LHON carriers demonstrated widespread decreased FA, increased RD and MD in bilateral white matter tracts of the brain. Moreover, no correlation was found between these altered diffusion metrics and ophthalmologic indices in LHON carriers. These results indicate that LHON-related mtDNA mutations could result in widespread brain white matter changes in asymptomatic LHON carriers.

In previous DTI studies, most of the recruited LHON patients are in the chronic stage of the disease, and patients generally show long-time damage in retina and optic nerves and manifest severe visual deficits. These studies have revealed white matter damage along the visual pathway and in some other white matter areas in LHON patients, which was usually interpreted as axonal degeneration secondary to the damage of retina and optic nerves [4, 35]. As supporting evidence, the reduced FA in the visual pathway is correlated with the decreased visual acuity in chronic LHON patients [35]. In the present study, however, we included LHON carriers who had LHON-related mtDNA mutations but did not have neuro-ophthalmologic symptoms. This sample is extremely suitable for investigating the occult brain white matter changes that resulted from LHON-related mtDNA mutations. In this special sample, we found extensive FA reduction, RD and MD increase in LHON carriers, suggesting that there are extensive microstructural changes in brain white matter. Moreover, the lack of correlations between diffusion and neuro-ophthalmologic changes in LHON carriers indicate primary alterations of brain white matter in these carriers.

The reduction of the FA indicates reduced anisotropy, which may be a result of increased RD and/or reduced AD [1]. The RD increase in LHON carriers was more extensive than FA reduction and should be the main reason behind FA

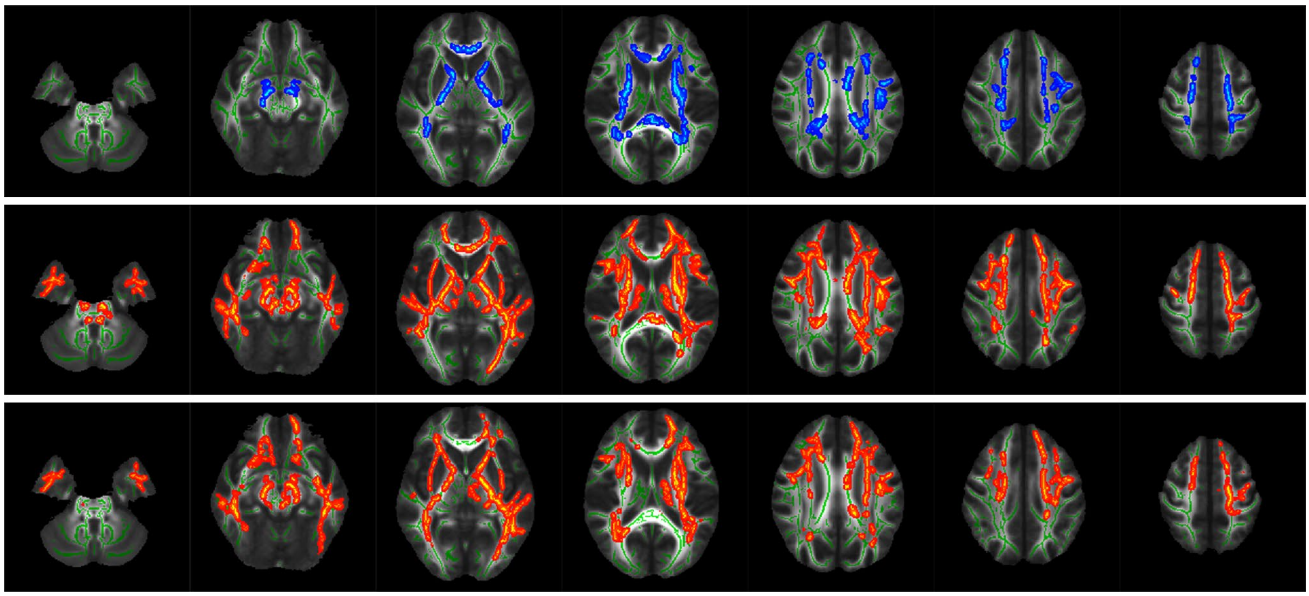

Fig. 1 Representative axial sections of voxel-wise TBSS analysis show reduced FA (upper row), increased RD(middle) and MD (bottom) values in LHON carriers than in healthy controls. The voxels with blue or light blue color represent those with significant reduction and the voxels with red or yellow color represent those with significant increase of DTI metrics in LHON carriers relative to healthy controls ($P < 0.05$, threshold-free cluster enhancement family-wise error corrected). The significant regions are thickened for better visibility. The white matter skeleton is shown in green (FA > 0.2). The background image is the mean FA map derived from all subjects

reduction and MD increase for AD showed no significant changes. Although the exact mechanisms remain unknown, two possible pathological processes may be related to the changes of diffusion metrics. One hypothesis is demyelination, which is the hallmark pathological change of multiple sclerosis [43]. This hypothesis is supported by the findings of the coexistence of multiple sclerosis and LHON-related mitochondrial DNA mutations in some patients [10, 11, 15, 20, 41, 46]. It is also supported by an electron microscopic analysis of optic tracts that shows the thinning of the myelin sheath in mouse mitochondrial DNA mutation model [29]. The second hypothesis is the redistribution of intracellular and extracellular water content caused by compensatory increase of mitochondrial biogenesis, with the indirect evidence of increased content of mitochondrial DNA [7, 40].

The significance of the thickening of the right-inferior-quadrant RNFL was weak, which failed to reach the changed meaningful *P* value level of 0.0125 for adjustment for multiplicity, though early studies showed that RNFL thickening is present in more than 1/3 of asymptomatic LHON carriers [14], and more diffuse in male carriers [50] and still present at acute phase of LHON [3]. The mechanism is likely to be a compensatory increase of mitochondrial biogenesis and/or the axonal stasis along the fibers [2].

The major limitation of this study is the relatively small sample size, which prevents us from dividing patients into several subgroups with enough sample size to observe the respective effect of potential confounding factors of gender, age and mutation types on brain white matter changes. However, we have tried our best to regress out the effects of age and gender.

In conclusion, to the best of our knowledge, this is the first study to explore the potential white matter microstructural changes of the brain in asymptomatic LHON carriers. We found extensive brain white matter changes in LHON carriers, indicating that LHON-related genetic mutations themselves might result in occult white matter changes in the brain.

Funding This work was supported by the Natural Science Foundation of China (81771818 and 81425013), and National Key Research and Development Program of China (2018YFC1314300 and 2017YFC0909201), and Natural Science Foundation of Tianjin (17JCYBJC29200).

Compliance with ethical standards

Conflicts of interest The authors declare that they have no conflicts of interest.

Ethical approval This research has been approved by the Ethics Committees of Tianjin Medical University General Hospital, Tianjin First Central Hospital, Zhengzhou University People's Hospital and Henan Provincial People's Hospital, and it has been performed in accordance with the ethical standards laid down in the 1964 Declaration of Helsinki and its later amendments.

Informed consent Informed consents from all subjects or their parents (for children less than 18 years old) were obtained before the study.

References

1. Alexander AL, Lee JE, Lazar M, Field AS (2007) Diffusion tensor imaging of the brain. Neurotherapeutics 4:316–329
2. Balducci N, Savini G, Cascavilla ML, La Morgia C, Triolo G, Giglio R, Carbonelli M, Parisi V, Sadun AA, Bandello F, Carelli V, Barboni P (2016) Macular nerve fibre and ganglion cell layer changes in acute Leber's hereditary optic neuropathy. Br J Ophthalmol 100:1232–1237
3. Barboni P, Carbonelli M, Savini G, Ramos Cdo V, Carta A, Berezovsky A, Salomao SR, Carelli V, Sadun AA (2010) Natural history of Leber's hereditary optic neuropathy: longitudinal analysis of the retinal nerve fiber layer by optical coherence tomography. Ophthalmology 117:623–627
4. Barcella V, Rocca MA, Bianchi-Marzoli S, Milesi J, Melzi L, Falini A, Pierro L, Filippi M (2010) Evidence for retrochiasmatic tissue loss in Leber's hereditary optic neuropathy. Hum Brain Mapp 31:1900–1906
5. Basser PJ, Mattiello J, LeBihan D (1994) Estimation of the effective self-diffusion tensor from the NMR spin echo. J Magn Reson Ser B 103:247–254
6. Bianco A, Bisceglia L, De Caro MF, Galeandro V, De Bonis P, Tullo A, Zoccolella S, Guerriero S, Petruzzella V (2018) Leber's hereditary optic neuropathy, intellectual disability and epilepsy presenting with variable penetrance associated to the m.3460G> A mutation and a heteroplasmic expansion of the microsatellite in MTRNR1 gene—case report. BMC Med Genet 19:129
7. Bianco A, Valletti A, Longo G, Bisceglia L, Montoya J, Emperador S, Guerriero S, Petruzzella V (2018) Mitochondrial DNA copy number in affected and unaffected LHON mutation carriers. BMC Res Notes 11:911
8. Carelli V, Valentino ML, Liguori R, Meletti S, Vetrugno R, Provini F, Mancardi GL, Bandini F, Baruzzi A, Montagna P (2001) Leber's hereditary optic neuropathy (LHON/11778) with myoclonus: report of two cases. J Neurol Neurosurg Psychiatry 71:813–816
9. d'Almeida OC, Mateus C, Reis A, Grazina MM, Castelo-Branco M (2013) Long term cortical plasticity in visual retinotopic areas in humans with silent retinal ganglion cell loss. NeuroImage 81:222–230
10. De Vries DD, Went LN, Bruyn GW, Scholte HR, Hofstra RM, Bolhuis PA, van Oost BA (1996) Genetic and biochemical impairment of mitochondrial complex I activity in a family with Leber hereditary optic neuropathy and hereditary spastic dystonia. Am J Hum Genet 58:703–711
11. Flanigan KM, Johns DR (1993) Association of the 11778 mitochondrial DNA mutation and demyelinating disease. Neurology 43:2720–2722
12. Funakawa I, Kato H, Terao A, Ichihashi K, Kawashima S, Hayashi T, Mitani K, Miyazaki S (1995) Cerebellar ataxia in patients with Leber's hereditary optic neuropathy. J Neurol 242:75–77
13. Grazina MM, Diogo LM, Garcia PC, Silva ED, Garcia TD, Robalo CB, Oliveira CR (2007) Atypical presentation of Leber's hereditary optic neuropathy associated to mtDNA 11778G> A point mutation—a case report. Eur J Paediatr Neurol 11:115–118
14. Guy J, Feuer WJ, Porciatti V, Schiffman J, Abukhalil F, Vandenbroucke R, Rosa PR, Lam BL (2014) Retinal ganglion cell dysfunction in asymptomatic G11778A: Leber hereditary optic neuropathy. Invest Ophthalmol Vis Sci 55:841–848
15. Harding AE, Riordan-Eva P, Govan GG (1995) Mitochondrial DNA diseases: genotype and phenotype in Leber's hereditary optic neuropathy. Muscle Nerve Suppl 3:S82–S84
16. Harding AE, Sweeney MG, Miller DH, Mumford CJ, Kellar-Wood H, Menard D, McDonald WI, Compston DA (1992) Occurrence of a multiple sclerosis-like illness in women who have a Leber's hereditary optic neuropathy mitochondrial DNA mutation. Brain J Neurol 115(Pt 4):979–989
17. Haselgrove JC, Moore JR (1996) Correction for distortion of echo-planar images used to calculate the apparent diffusion coefficient. Magn Reson Med 36:960–964
18. Huoponen K, Vilkki J, Aula P, Nikoskelainen EK, Savontaus ML (1991) A new mtDNA mutation associated with Leber hereditary optic neuroretinopathy. Am J Hum Genet 48:1147–1153
19. Jancic J, Dejanovic I, Radovanovic S, Ostojic J, Kozic D, Duric-Jovicic M, Samardzic J, Cetkovic M, Kostic V (2016) White matter changes in two Leber's hereditary optic neuropathy pedigrees: 12-year follow-up. Ophthalmologica 235:49–56
20. Jansen PH, van der Knaap MS, de Coo IF (1996) Leber's hereditary optic neuropathy with the 11 778 mtDNA mutation and white matter disease resembling multiple sclerosis: clinical, MRI and MRS findings. J Neurol Sci 135:176–180
21. Johns DR, Smith KH, Miller NR (1992) Leber's hereditary optic neuropathy. Clinical manifestations of the 3460 mutation. Arch Ophthalmol (Chicago, Ill: 1960) 110:1577–1581
22. Johnsson P, Lundqvist C, Lindgren A, Ferencz I, Alling C, Stahl E (1995) Cerebral complications after cardiac surgery assessed by S-100 and NSE levels in blood. J Cardiothorac Vasc Anesth 9:694–699
23. Kermode AG, Moseley IF, Kendall BE, Miller DH, MacManus DG, McDonald WI (1989) Magnetic resonance imaging in Leber's optic neuropathy. J Neurol Neurosurg Psychiatry 52:671–674
24. Klivenyi P, Karg E, Rozsa C, Horvath R, Komoly S, Nemeth I, Turi S, Vecsei L (2001) alpha-Tocopherol/lipid ratio in blood is decreased in patients with Leber's hereditary optic neuropathy and asymptomatic carriers of the 11778 mtDNA mutation. J Neurol Neurosurg Psychiatry 70:359–362
25. La Morgia C, Achilli A, Iommarini L, Barboni P, Pala M, Olivieri A, Zanna C, Vidoni S, Tonon C, Lodi R, Vetrugno R, Mostacci B, Liguori R, Carroccia R, Montagna P, Rugolo M, Torroni A, Carelli V (2008) Rare mtDNA variants in Leber hereditary optic neuropathy families with recurrence of myoclonus. Neurology 70:762–770
26. Le Bihan D (2003) Looking into the functional architecture of the brain with diffusion MRI. Nat Rev Neurosci 4:469–480
27. Le Bihan D, Johansen-Berg H (2012) Diffusion MRI at 25: exploring brain tissue structure and function. NeuroImage 61:324–341
28. Li Y, Li J, Jia X, Xiao X, Li S, Guo X (2017) Genetic and clinical analyses of DOA and LHON in 304 chinese patients with suspected childhood-onset hereditary optic neuropathy. PloS One 12:e0170090
29. Lin CS, Sharpley MS, Fan W, Waymire KG, Sadun AA, Carelli V, Ross-Cisneros FN, Baciu P, Sung E, McManus MJ, Pan BX, Gil DW, Macgregor GR, Wallace DC (2012) Mouse mtDNA mutant model of Leber hereditary optic neuropathy. Proc Natl Acad Sci USA 109:20065–20070
30. Lodi R, Montagna P, Cortelli P, Iotti S, Cevoli S, Carelli V, Barbiroli B (2000) 'Secondary' 4216/ND1 and 13708/ND5 Leber's hereditary optic neuropathy mitochondrial DNA mutations do not further impair in vivo mitochondrial oxidative metabolism when associated with the 11778/ND4 mitochondrial DNA mutation. Brain J Neurol 123(Pt 9):1896–1902
31. Lodi R, Taylor DJ, Tabrizi SJ, Kumar S, Sweeney M, Wood NW, Styles P, Radda GK, Schapira AH (1997) In vivo skeletal muscle mitochondrial function in Leber's hereditary optic neuropathy assessed by 31P magnetic resonance spectroscopy. Ann Neurol 42:573–579
32. Mackey D, Howell N (1992) A variant of Leber hereditary optic neuropathy characterized by recovery of vision and by an unusual mitochondrial genetic etiology. Am J Hum Genet 51:1218–1228
33. Manners DN, Rizzo G, La Morgia C, Tonon C, Testa C, Barboni P, Malucelli E, Valentino ML, Caporali L, Strobbe D, Carelli V,

Lodi R (2015) Diffusion tensor imaging mapping of brain white matter pathology in mitochondrial optic neuropathies. Am J Neuroradiol 36:1259–1265
34. Meire FM, Van Coster R, Cochaux P, Obermaier-Kusser B, Candaele C, Martin JJ (1995) Neurological disorders in members of families with Leber's hereditary optic neuropathy (LHON) caused by different mitochondrial mutations. Ophthalmic Genet 16:119–126
35. Milesi J, Rocca MA, Bianchi-Marzoli S, Petrolini M, Pagani E, Falini A, Comi G, Filippi M (2012) Patterns of white matter diffusivity abnormalities in Leber's hereditary optic neuropathy: a tract-based spatial statistics study. J Neurol 259:1801–1807
36. Nakaso K, Adachi Y, Fusayasu E, Doi K, Imamura K, Yasui K, Nakashima K (2012) Leber's hereditary optic neuropathy with olivocerebellar degeneration due to G11778A and T3394C mutations in the mitochondrial DNA. J Clin Neurol (Seoul Korea) 8:230–234
37. Newman NJ, Lott MT, Wallace DC (1991) The clinical characteristics of pedigrees of Leber's hereditary optic neuropathy with the 11778 mutation. Am J Ophthalmol 111:750–762
38. Nichols TE, Holmes AP (2002) Nonparametric permutation tests for functional neuroimaging: a primer with examples. Hum Brain Mapp 15:1–25
39. Nikoskelainen EK, Marttila RJ, Huoponen K, Juvonen V, Lamminen T, Sonninen P, Savontaus ML (1995) Leber's "plus": neurological abnormalities in patients with Leber's hereditary optic neuropathy. J Neurol Neurosurg Psychiatry 59:160–164
40. Nishioka T, Soemantri A, Ishida T (2004) mtDNA/nDNA ratio in 14484 LHON mitochondrial mutation carriers. J Hum Genet 49:701–705
41. Olsen NK, Hansen AW, Norby S, Edal AL, Jorgensen JR, Rosenberg T (1995) Leber's hereditary optic neuropathy associated with a disorder indistinguishable from multiple sclerosis in a male harbouring the mitochondrial DNA 11778 mutation. Acta Neurol Scand 91:326–329
42. Ostojic J, Jancic J, Kozic D, Semnic R, Koprivsek K, Prvulovic M, Kostic V (2009) Brain white matter 1 H MRS in Leber optic neuropathy mutation carriers. Acta Neurol Belg 109:305–309
43. Popescu BF, Pirko I, Lucchinetti CF (2013) Pathology of multiple sclerosis: where do we stand? Continuum (Minneap Minn) 19:901–921
44. Qin W, Zhang M, Piao Y, Guo D, Zhu Z, Tian X, Li K, Yu C (2012) Wallerian degeneration in central nervous system: dynamic associations between diffusion indices and their underlying pathology. PloS One 7:e41441
45. Rance G, Kearns LS, Tan J, Gravina A, Rosenfeld L, Henley L, Carew P, Graydon K, O'Hare F, Mackey DA (2012) Auditory function in individuals within Leber's hereditary optic neuropathy pedigrees. J Neurol 259:542–550
46. Riordan-Eva P, Sanders MD, Govan GG, Sweeney MG, Da Costa J, Harding AE (1995) The clinical features of Leber's hereditary optic neuropathy defined by the presence of a pathogenic mitochondrial DNA mutation. Brain J Neurol 118(Pt 2):319–337
47. Rocca MA, Valsasina P, Pagani E, Bianchi-Marzoli S, Milesi J, Falini A, Comi G, Filippi M (2011) Extra-visual functional and structural connection abnormalities in Leber's hereditary optic neuropathy. PloS One 6:e17081
48. Sadun AA, Win PH, Ross-Cisneros FN, Walker SO, Carelli V (2000) Leber's hereditary optic neuropathy differentially affects smaller axons in the optic nerve. Trans Am Ophthalmol Soc 98:223–232 (discussion 232–225)
49. Salomao SR, Berezovsky A, Andrade RE, Belfort R Jr, Carelli V, Sadun AA (2004) Visual electrophysiologic findings in patients from an extensive Brazilian family with Leber's hereditary optic neuropathy. Doc Ophthalmol Adv Ophthalmol 108:147–155
50. Savini G, Barboni P, Valentino ML, Montagna P, Cortelli P, De Negri AM, Sadun F, Bianchi S, Longanesi L, Zanini M, Carelli V (2005) Retinal nerve fiber layer evaluation by optical coherence tomography in unaffected carriers with Leber's hereditary optic neuropathy mutations. Ophthalmology 112:127–131
51. Smith SM, Jenkinson M, Johansen-Berg H, Rueckert D, Nichols TE, Mackay CE, Watkins KE, Ciccarelli O, Cader MZ, Matthews PM, Behrens TE (2006) Tract-based spatial statistics: voxelwise analysis of multi-subject diffusion data. NeuroImage 31:1487–1505
52. Smith SM, Nichols TE (2009) Threshold-free cluster enhancement: addressing problems of smoothing, threshold dependence and localisation in cluster inference. NeuroImage 44:83–98
53. Ventura DF, Quiros P, Carelli V, Salomao SR, Gualtieri M, Oliveira AG, Costa MF, Berezovsky A, Sadun F, de Negri AM, Sadun AA (2005) Chromatic and luminance contrast sensitivities in asymptomatic carriers from a large Brazilian pedigree of 11778 Leber hereditary optic neuropathy. Invest Ophthalmol Vis Sci 46:4809–4814
54. Vergani L, Martinuzzi A, Carelli V, Cortelli P, Montagna P, Schievano G, Carrozzo R, Angelini C, Lugaresi E (1995) MtDNA mutations associated with Leber's hereditary optic neuropathy: studies on cytoplasmic hybrid (cybrid) cells. Biochem Biophys Res Commun 210:880–888
55. Wallace DC, Singh G, Lott MT, Hodge JA, Schurr TG, Lezza AM, Elsas LJ II, Nikoskelainen EK (1988) Mitochondrial DNA mutation associated with Leber's hereditary optic neuropathy. Science 242:1427–1430
56. Wheeler-Kingshott CA, Cercignani M (2009) About "axial" and "radial" diffusivities. Magn Reson Med 61:1255–1260
57. Yardan T, Cevik Y, Donderici O, Kavalci C, Yilmaz FM, Yilmaz G, Vural K, Yuzbasioglu Y, Gunaydin YK, Sezer AA (2009) Elevated serum S100B protein and neuron-specific enolase levels in carbon monoxide poisoning. Am J Emerg Med 27:838–842
58. Yee KM, Ross-Cisneros FN, Lee JG, Da Rosa AB, Salomao SR, Berezovsky A, Belfort R Jr, Chicani F, Moraes-Filho M, Sebag J, Carelli V, Sadun AA (2012) Neuron-specific enolase is elevated in asymptomatic carriers of Leber's hereditary optic neuropathy. Invest Ophthalmol Vis Sci 53:6389–6392